JOURNAL OF CHEMICAL & ENGINEERING DATA

ARTICLE

pubs.acs.org/jced

Isobaric Specific Heat Capacity Measurement for Kerosene RP-3 in the Near-Critical and Supercritical Regions

H. W. Deng,[†] K. Zhu,[*,†] G. Q. Xu,[†] Z. Tao,[†] C. B. Zhang,[†] and G. Z. Liu[‡]

[†]National Key Laboratory of Science and Technology on Aero-Engine Aero-thermodynamics, School of Jet Propulsion, Beihang University, Beijing, 100191, P. R. China

[‡]School of Chemical Engineering and Technology, Tianjin University, Tianjin, 300072, P. R. China

ABSTRACT: The isobaric specific heat capacity of kerosene RP-3 was experimentally measured using a vacuum flow-calorimeter in the near-critical and supercritical regions. During the experiments, the qualitative temperature changed from (292.1 to 823.9) K, and the operation pressure changed from (2.40 to 5.98) MPa. The operation pressure, fuel inlet and outlet bulk temperatures, mass flow rate, and heat power were measured using a pressure gauge transducer, K-type sheathed thermocouples, a Coriolis-force flow meter, and current and voltage meters, respectively. The estimated uncertainty of the measurement was lower than 2.11 %. The expanded accuracy of the measured method for the low temperature region was verified by the water at the pressure of 3.01 MPa; the high-temperature region was verified by comparing the temperatures calculated from C_p integrating enthalpy with the temperatures measured in the experiments.

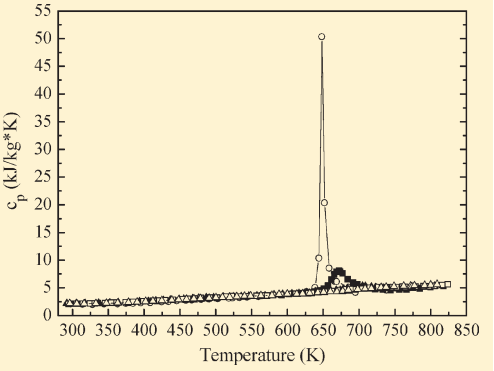

INSTRUCTION

In modern aerospace engineering, the turbine components suffer thermal stress and heat loads, which reduce the turbine performance and lifetime. As the compressor pressure ratio increases, the temperature of the cooling air delivered from the compressor to the turbine vane and blades increases. Consequently, the increased cooling air temperature causes weaker cooling efficiency. The cooled cooling air (CCA), which uses the fuel as the coolant, is a new cooling method and has been widely used recently.[1] The fuel is heated while the coolant air is cooled. The pressure of a typical aircraft fuel system is about (3.45 to 6.89) MPa;[2] this value goes beyond the critical pressure of fuel.[3] When the fuel flows through the heat exchanger, the fuel temperature continually increases as the fuel absorbs the heat from the cooling air. The fuel undergoes a transition through its pseudocritical temperature T_{pc} (where the specific heat capacity reaches the peak value at the fixed operation pressure) while flowing through the heat exchanger. Previous literature indicated that the heat transfer characteristics of supercritical fluid changed dramatically near the pseudocritical temperature, and flow oscillation occurred due to the thermal properties.[4−14] Therefore, the thermal properties under different operating pressures are crucial for the heat transfer and flow characteristics analysis of supercritical fluid.

The specific heat capacity of single-component fluids has been measured using a flow calorimeter[15−19] or calculated from the Helmholtz energy state equations for typical fluids.[20−22] A flow calorimeter may be more suitable than a static one for measuring heat capacity of fluids at high temperatures and pressures because it can simulate the real fluid status more accurately and also provide a more uniform temperature profile. These are crucial for isobaric specific heat capacity C_p measurement.

The complex components of the propellant used in rocket and aircraft engines will result in more complicated thermal properties than those of the pure component fluids. Many researchers have investigated the thermal properties of rocket propellant RP-1[23−25] and RP-2[25] with surrogate mixture models[23−25] and static experiments,[24] respectively. The surrogate mixture model method, aimed at the thermal properties, depends on large amounts of experimental data and known accurate fuel components. The results show that the thermal properties of fuels depend on the individual components.

The kerosene RP-3, the most popular jet fuel used in aeronautical engines of China, has unique components compared to other kerosenes.[26] The isobaric specific heat capacity of kerosene RP-3 has not been measured or published. The shortage of information about the thermal properties of RP-3 limits the application of engine thermal management, especially the application of CCA technology.

The main objective of this work was to measure the isobaric specific heat capacity of kerosene RP-3 in the near-critical and supercritical regions using a new reliable vacuum adiabatic flow calorimeter. During the experiments, the operation pressure was varied from (2.40 to 5.98) MPa, and the temperature of fuel was varied from (292.1 to 823.9) K. The operating conditions covered near-critical and supercritical conditions.

Received: June 18, 2011
Accepted: November 27, 2011
Published: December 21, 2011

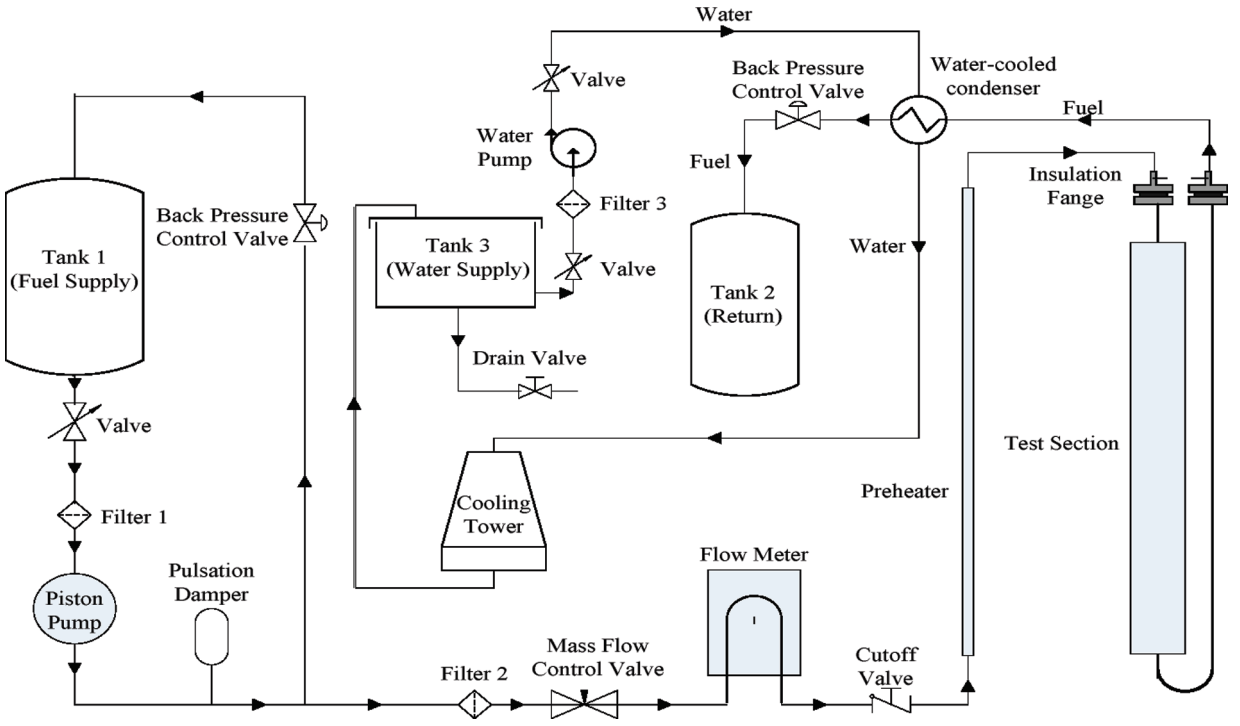

Figure 1. Schematic of the experimental system.

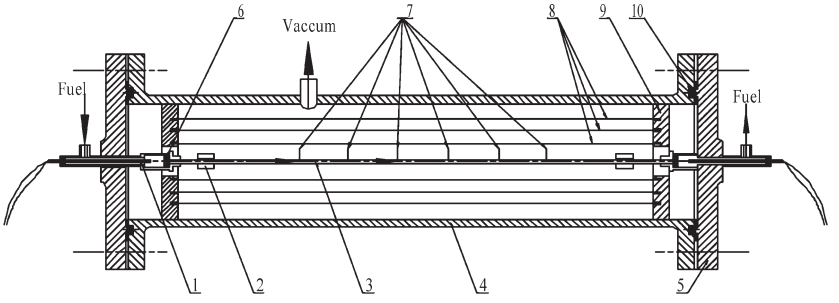

Figure 2. Schematic of the test section: 1, thermocouples; 2, electrical heating power connection; 3, test tube; 4, vacuum jacket; 5, flange; 6, filter net; 7, wall temperature thermocouples; 8, radiation shield; 9, shield fixer; 10, gasket.

FACILITY AND MATERIALS

Experimental System. Figure 1 shows the experimental system, which consists of a preparative system, a test section, and a holding tank. Some of this experimental equipment are similar to those in published literature.[27]

The preparative system prepares the fuel to the desired experimental conditions. Initially, the pressure of the fuel in tank 1 is increased to 16 MPa by a piston pump (2J-Z 104/16, Ailipu). Then the prepressed fuel goes into an airbag pulsation (NXQ-L04/16-H, Tianyuan) to reduce the pressure pulsation below 5 % of the test section inlet pressure. The fuel out from the airbag is then divided into major path fuel and otiose fuel: the mass rate of major path fuel is regulated by the mass flow control valve and measured by a Coriolis-force flow meter (DMF-1-1, Sincerity) with an accuracy of ± 0.2 %; the otiose fuel, whose mass flow rate is controlled by a back pressure control value (SS-426F3, Xiongchuan), is collected for reuse. To achieve the required fuel temperature of the test section, the prepressurized major path fuel is heated with proper heat flux by a current power (maximum 20 kW) on the stainless tube in the preheater section. The heated fuel then enters into the test section for isobaric specific heat capacity measurement. The pressure of the fuel in the test section is controlled by a back pressure valve (0 to 15) MPa and measured by a digital pressure gauge (3051CA4, Rosemount) with a measuring ability accuracy of ± 0.065 %. After testing, the fuel is cooled below 310 K by a water-cooled condenser and collected into tank 2.

Figure 2 schematically describes the details of the test section structure of the isobaric specific heat capacity flow-calorimeter. The inside and outside diameters of the heating stainless tube are 1.8 mm and 2.2 mm, respectively; the length of the tube, not including the entrance length (50 mm) and exit length (50 mm), is 800 mm. The heating tube is placed in a nearly vacuum environment (nearly 80 Pa) vertically. The required heat flux of the test section is achieved by heating the stainless tube directly using low voltage alternating current. The heating voltage and current are measured with a voltage meter (XST/C-H1VA1-VON, Kunlun) with an accuracy of ± 0.2 % and an ampere meter (XSP1C/A-HiT1A1SO, Kunlun) with an accuracy of ± 0.2 %.

dx.doi.org/10.1021/je200523a |J. Chem. Eng. Data 2012, 57, 263–268

The differential temperature and inlet and outlet fuel temperatures are measured by K-type sheathed thermocouples (φ = 1.5 mm) respectively via the bulk temperature mixed cavity. The six K-type wall temperature thermocouples (φ = 0.1 mm) are used to estimate the heat loss of the calorimeter. All thermocouples have been calibrated in the constant temperature bath, and the measurement accuracy is ± 0.2 K in the temperature region from (293.15 to 573.15) K and ± 0.4 % from (573.15 to 873.15) K. The data are recorded automatically using the model ADAM4018 and transmitted to the computer with the model ADAM4520.

To obtain reliable results, it is necessary to reduce heat loss. During measurements, heat loss is reduced using the following methods: (a) Heat loss by convection is reduced by mounting the calorimeter in a vacuum jacket (nearly 80 Pa) and covering the surface with isothermal material Aspen aerogels (thermal conductivity λ = 0.012 $W \cdot m^{-1} \cdot K^{-1}$). (b) Heat loss by conduction is reduced by using a tube as a test section and keeping the small temperature difference between the inlet and the outlet of the test section (about 10 K). (c) Heat loss by radiation is reduced by three radiation shields covering the entire test tube and are fixed together at each end of the vacuum jacket. Heat loss cannot be avoided completely using the previous method, and the correction for heat loss will be introduced in the following section.

Materials. The kerosene RP-3 is purchased from China Fuel Supply Co., Ltd. The main components have been evaluated (Agilent GC6890-MS5975) and reported.[27] In our previous work, the critical point of RP-3 sample was measured as 2.33 MPa and 644.35 K due to the obviously critical opalescence phenomenon in the visualized experiment.

THEORY

The measurement of isobaric specific heat capacity C_p is conducted by heating a constant mass flow rate sample $\dot{m}$ in the calorimeter from bulk temperature T_{in} to T_{out} by the electric heating power Φ under the fixed inlet pressure. The C_p can be calculated in the small differential temperature of T_{in} and T_{out} region by using the energy-balance equation as follows:

$$\Phi = UI = \dot{m} \cdot \int_{T_{in}}^{T_{out}} C_p \, dT + \Phi_{loss} = \dot{m} \cdot C_p|_T \cdot \Delta T + \Phi_{loss} \quad (1)$$

where Φ_{loss}, U, and I are the heating power loss, voltage, and electrical current of the experimental test section, respectively. ΔT is the measured test tube inlet and outlet differential bulk temperature, and T = 1/2 (T_{out} + T_{in}) is the qualitative temperature of the isobaric specific heat capacity during the measurement.

To obtain the heat power loss Φ_{loss}, which is a function of the differential temperature between the tube outer wall temperature $T_{wx,out}$ and environmental temperature T_{surr}, the individual heat loss experiment is taken by heating the calorimeter without an inner fluid. Consequently, the Φ_{loss} equation can be established as eq 2.

$$\Phi_{loss} = U'I' = f(T_{wx,out} - T_{surr}) \quad (2)$$

where I' and U' are the electric current and voltage, respectively, in the heat loss experiment.

During the C_p measurements, U, I, $\dot{m}$, and (T_{out} − T_{in}) are measured by a voltmeter, ampere meter, flow meter, and differential temperature thermocouples. Table 1 shows the experimental uncertainty of the direct measurements. The relatively combined expended uncertainty of isobaric specific heat capacity measurements is about ± 2.11 %, according to data in Table 1.

Table 1. Direct Measurement Uncertainty

direct measurement	measuring uncertainty
mass flow rate $\dot{m}$	± 0.2 %
operation pressure p	± 0.065 %
heating electric current I	± 0.2 %
heating electric voltage U	± 0.2 %
heat loss electric current I'	± 0.2 %
heat loss electric voltage U'	± 0.2 %
rube outer wall temperature $T_{w,out}$	± 0.2 K, (293 to 573) K
	± 0.4 %, (573 to 873) K
duel inlet and outlet bulk temperature T_f	± 0.2 K, (293 to 573) K
	± 0.4 %, (573 to 873) K
qualitative temperature T	± 0.28 K, (293 to 573) K
	± 0.57 %, (573 to 873) K
inlet and outlet differential temperature ΔT	± 0.2 K, (293 to 573) K
	± 0.4 %, (573 to 873) K

Table 2. Capacity of Experimental Results and Published Data[20]

T	$C_{p,exp}$	$C_{p,lit}$	
K	$kJ \cdot kg^{-1} \cdot K^{-1}$	$kJ \cdot kg^{-1} \cdot K^{-1}$	deviation %
288.0	4.38	4.18	4.7
291.6	4.22	4.18	0.9
299.6	3.97	4.17	−4.8
318.2	4.01	4.17	−3.8
337.2	4.02	4.18	−3.8
352.8	4.24	4.19	1.1
365.9	4.04	4.20	−3.9
378.2	4.11	4.22	−2.4
390.9	4.10	4.24	−3.1
404.4	4.07	4.26	−4.6
422.9	4.40	4.30	2.3

RESULTS AND DISCUSSION

Accuracy and Reliability in the Low-Temperature Region. To confirm the accuracy and reliability of the method in this paper, the isobaric specific heat capacity of water was measured using the method of section 3. In the experiment, the pressure was fixed at 3.01 MPa, and the temperature of water changed from (288.0 to 422.9) K. The measured capacity was compared with published data (uncertainty of ± 0.1 %) in Table 2.[20]

Table 2 illustrates that the average absolute deviation AAD (as eq 3) of the isobaric specific heat capacity between the measured data and the published data is 3.2 %, and the maximum absolute deviation MAD (as eq 4) of the test measurement is about 4.8 %. The deviation may be caused by the axial heat conduct and high Φ_{loss}/Φ in the low-temperature region.

$$AAD = (1/n) \sum_{i=1}^{n} \left(\left| \frac{C_{p,exp,i}}{C_{p,lit,i}} - 1 \right| \right) \qquad n = 11 \quad (3)$$

dx.doi.org/10.1021/je200523a |J. Chem. Eng. Data 2012, 57, 263–268

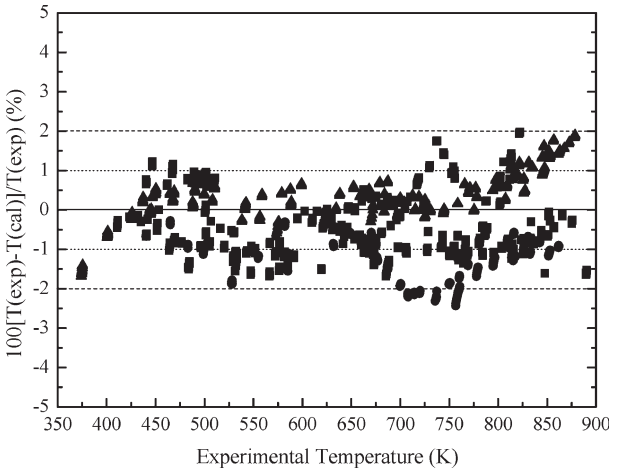

Figure 3. Comparison of the experimental measured temperature against calculated temperature at different pressures. ▲, p = 3.02 MPa; ●, p = 4.02 MPa; ■, p = 4.98 MPa.

$$\mathrm{MAD} = \mathrm{MAX}\left(\left|\left(\frac{C_{p,\exp,t}}{C_{p,\mathrm{lit},t}} - 1\right)\right|\right) \quad (4)$$

Accuracy and Reliability in the High-Temperature Region. To confirm the isobaric specific heat capacity C_p measurement accuracy in the high-temperature region, another method has been proposed. In the small differential temperature region i, the enthalpy H and C_p can be regarded as changing linearly with the temperature, so that the fuel enthalpy can be obtained by the following equation.

$$H(T_i) - H(T_{i-1}) = \int_{T_{i-1}}^{T_i} C_p(T)\,\mathrm{d}T = C_p|_{T_{i-1}}^{T_i} \cdot (T_i - T_{i-1}) \quad (5)$$

where $H(T_i)$ and $H(T_{i-1})$ are the enthalpies at fuel bulk temperature T_i and T_{i-1}, respectively, and $C_p(T)$ is the measured isobaric heat capacity in this paper. Integrating the left and right side of the eq 5 and considering the system inlet fuel enthalpy to be zero, we will obtain the fuel enthalpy function $H(T)$, whose inverse function $H^{-1}(T)$ will be used to calculate the heaters' outlet fuel temperature with the measured heating power Φ_{pre} and mass flow rate $\dot{m}$.

Figure 3 indicates the comparison of the experimental measured fuel outlet temperatures and calculated fuel outlet temperatures using the above method. As shown in Figure 3, 2304 data points out of 2348 points (98.13 %) are in the ± 2 % error band, and 1622 points are within the ± 1 % error band. The errors are mainly caused by the thermocouple measurement and the integrating process of calculation. The results manifest that the uncertainty of the calorimeter is stable in both low- and high-temperature regions and the isobaric specific heat capacity measurement is believable in the high-temperature and high-pressure regions for research and engineering applications.

Isobaric Specific Heat Capacity Measurement of RP-3. Using the mentioned method in section 3, the isobaric specific heat capacity under different temperatures was measured. During the experiments, the qualitative temperature changed from (292.1 to 823.9) K in one fixed pressure [(2.40, 3.02, 4.02,

Table 3. Isobaric Specific Heat Capacity Measurement of RP-3

T/K	C_p/kJ·kg^{-1}·K^{-1}	T/K	C_p/kJ·kg^{-1}·K^{-1}	T/K	C_p/kJ·kg^{-1}·K^{-1}
		p/MPa = 2.40			
297.3	2.12	479.7	2.91	666.0	6.19
314.3	2.05	490.6	2.98	668.7	6.14
328.1	2.04	502.8	3.05	686.2	5.11
344.1	2.07	518.2	3.16	695.0	4.21
363.0	2.13	523.4	3.19	710.1	4.92
374.7	2.17	533.1	3.24	724.7	4.92
384.6	2.21	543.7	3.33	737.8	4.61
395.3	2.27	559.5	3.42	750.2	5.02
408.7	2.35	626.9	4.29	768.2	5.00
424.5	2.46	638.5	5.05	777.5	5.11
434.3	2.55	644.0	10.38	792.0	5.28
445.7	2.66	648.2	50.35	802.0	5.37
458.5	2.76	652.0	20.37		
466.6	2.84	658.4	8.58		
		p/MPa = 3.02			
297.1	2.14	614.9	3.95	684.4	6.54
335.4	2.20	621.1	4.05	691.7	5.96
378.0	2.33	630.2	4.17	698.0	5.64
418.4	2.60	637.5	4.34	707.8	5.14
457.9	2.85	644.9	4.56	714.5	4.95
464.1	2.91	651.0	4.86	722.7	4.76
471.0	2.97	656.9	5.44	733.5	4.73
480.5	3.02	661.3	6.49	744.2	4.64
490.6	3.09	665.5	7.46	756.5	4.68
501.9	3.15	668.5	7.86	766.6	4.71
537.5	3.40	672.1	8.09	784.7	4.86
561.4	3.54	673.9	7.92	799.9	5.09
592.1	3.72	677.3	7.65	818.0	5.35
		p/MPa = 4.02			
292.1	2.18	511.0	3.34	689.5	5.08
305.3	2.18	524.4	3.37	691.9	5.18
317.7	2.20	535.7	3.39	697.7	5.34
336.6	2.23	546.0	3.50	704.7	5.32
352.2	2.29	557.4	3.56	708.6	5.25
363.9	2.33	568.8	3.58	717.2	5.16
378.4	2.40	581.4	3.72	722.7	5.05
393.8	2.49	593.4	3.84	724.5	4.99
406.0	2.58	606.1	3.95	729.6	4.88
416.3	2.62	616.1	3.99	731.9	4.94
427.0	2.70	626.8	4.16	733.9	4.90
436.6	2.79	638.7	4.29	737.0	4.90
449.1	2.89	654.9	4.29	744.2	4.89
455.4	2.96	661.1	4.33	757.8	4.88
467.6	3.07	668.2	4.55	765.9	4.89
476.1	3.13	673.5	4.57	774.1	4.94
486.7	3.23	677.6	4.74	792.9	5.10
496.9	3.24	683.3	4.88	805.6	5.31
		p/MPa = 4.98			
294.6	2.10	331.4	2.20	374.4	2.41
305.9	2.12	345.4	2.26	384.9	2.48

dx.doi.org/10.1021/je200523a |J. Chem. Eng. Data 2012, 57, 263–268

Table 3. Continued

T	C_p	T	C_p	T	C_p
K	kJ·kg^{-1}·K^{-1}	K	kJ·kg^{-1}·K^{-1}	K	kJ·kg^{-1}·K^{-1}
314.6	2.15	354.0	2.30	399.0	2.57
325.0	2.18	361.6	2.33	413.0	2.65
		p/MPa = 4.98			
421.6	2.70	580.6	3.71	715.1	5.03
429.8	2.76	591.5	3.77	726.7	5.10
440.5	2.85	602.3	3.90	732.1	5.11
453.6	2.97	611.6	3.96	737.9	5.11
461.2	3.03	629.3	4.05	746.9	5.15
470.3	3.09	634.4	4.07	752.6	5.14
479.1	3.18	643.6	4.19	760.7	5.20
492.4	3.20	652.6	4.27	764.7	5.18
502.1	3.24	662.6	4.42	779.1	5.22
514.2	3.42	671.9	4.60	790.0	5.32
522.9	3.51	677.6	4.41	798.7	5.28
533.8	3.44	681.7	4.74	805.4	5.35
544.5	3.48	686.5	4.56	816.4	5.48
557.0	3.58	688.3	4.78	823.9	5.64
564.8	3.61	695.5	4.69		
572.1	3.63	704.8	4.84		
		p/MPa = 5.98			
296.5	2.17	500.1	3.23	677.1	4.43
306.0	2.14	509.4	3.29	685.0	4.59
316.3	2.14	519.4	3.35	698.1	4.71
332.9	2.17	529.5	3.44	708.5	4.84
347.4	2.21	540.3	3.50	717.5	4.88
363.3	2.28	548.7	3.54	730.7	5.07
378.2	2.37	563.1	3.59	737.6	5.10
390.3	2.43	578.6	3.63	748.9	5.28
402.1	2.52	588.5	3.83	762.3	5.31
412.4	2.60	600.0	3.88	771.8	5.31
424.9	2.69	613.3	3.88	773.7	5.24
438.7	2.78	621.1	3.95	777.4	5.41
448.5	2.87	631.1	4.03	791.6	5.46
459.3	2.94	642.4	4.11	799.8	5.53
469.3	3.01	650.3	4.20	808.8	5.63
478.7	3.09	660.1	4.29		
490.8	3.14	669.3	4.33		

4.98, and 5.98) MPa]. The isobaric specific heat capacity in different conditions is shown in Table 3.

Figure 4 presents the experimental isobaric specific heat capacity of RP-3 in the C_p-T plane under various operation pressures. To indicate the isobaric heat capacity clearly, the results have been divided into two figures (a) for all of the pressures and (b) for pressures from (3.02 to 5.98) MPa. As shown in Figure 4, the measured C_p variation demonstrates a similar tendency with other studies in the near- and supercritical regions.[15−17,20−22]

According to Figure 4, in the relative low temperature region, the isobaric heat capacity of kerosene RP-3 increases monotonically with an increasing temperature for constant pressure; the pressure does not influence the isobaric heat capacity of kerosene RP-3. This means the isobaric specific heat capacity is mainly influenced by the fluid temperature. When the temperature rises

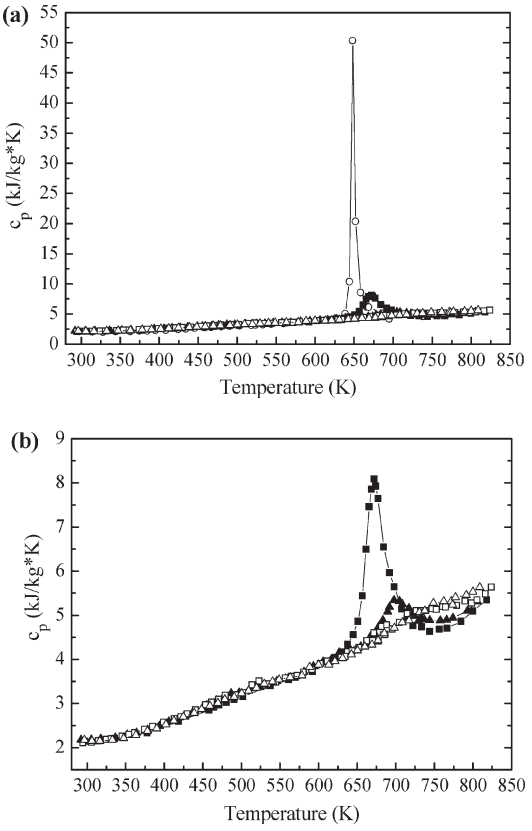

Figure 4. Isobaric specific heat capacity of RP-3 under variable operation pressures. ○, p = 2.40 MPa; ■, p = 3.02 MPa; ▲, p = 4.02 MPa; □, p = 4.98 MPa; △, p = 5.98 MPa. (a) All measured pressures; (b) measured pressures from (3.02 to 5.98) MPa.

to T/T_{pc} = 0.92 to 0.95, the isobaric specific heat capacity increases dramatically; it reaches the peak value within a petty temperature region and then decreases sharply. The sharp change occurs within a narrow temperature region (≈50 K). After that, the C_p increases smoothly with a similar increasing trend of the low-temperature region. The peak behavior is not obvious at the relative high pressures [(4.98 and 5.98) MPa]. These trends are consistent with the conclusions from previous studies of supercritical fluids.[15,17,21,22]

Additionally, for the fluid under near-critical and supercritical pressure, the temperature where the fluid thermal properties change dramatically, especially isobaric specific heat capacity, is considered to be the critical temperature and pseudocritical temperature, respectively. Hence, the results also indicate the pseudocritical temperature for different pressures. It manifests that the largest heat capacity variation occurs at the temperature of 648.2 K under the pressure of 2.40 MPa, which is close to the published critical point (645.3 K, 2.319 MPa).[28] When the pressure is 3.02 MPa, the pseudocritical temperature is 672.1 K; the pseudocritical temperature increases to 697.7 K when the operation pressure is 4.02 MPa. When the operation pressure exceeds 4.98 MPa, the pseudocritical temperature is not observable in the experimental conditions.

■ CONCLUSIONS

A feasible flow apparatus for the accurate isobaric heat capacity measurement of a single phase fluid at temperatures up to 823.9 K

and pressures up to 5.98 MPa has been constructed and tested. First, the method was tested at the pressure of 3.01 MPa with water in a low-temperature range, (288.0 to 422.9) K. The measurement average absolute deviation (AAD) is 3.2 %, and the maximum absolute deviation (MAD) is 4.8 %. Second, the accuracy of the isobaric specific heat capacity measurement in the high-temperature region was evaluated. This was done by comparing the experimentally determined fuel outlet temperatures to the calculated ones which were based on their enthalpy. Third, the kerosene RP-3 isobaric heat capacity data have been experimentally obtained at temperatures in the range (292.1 to 823.9) K and pressures in the range of (2.40 to 5.98) MPa. Moreover, the critical (648.2 K) and pseudocritical temperatures (672.1 K, 697.7 K) under different pressures [(2.40, 3.02, and 4.02) MPa, respectively] have been obtained from the isobaric specific heat capacity measurement. These quantities are invaluable for research and engineering design applications at near-critical and supercritical regions.

AUTHOR INFORMATION

Corresponding Author

*E-mail: kun-zhu@sjp.buaa.edu.cn. Fax: +86-10-82314545.

Funding Sources

This work is supported by the China National Nature Science Foundation (Contract No. 50676005).

ACKNOWLEDGMENT

The authors wish to thank the technical assistance of Guozhu Liu from Tianjin University, P.R. China, and Haiwang Li from the NanYang Technological University, Singapore.

REFERENCES

(1) Bruening, G. B.; Chang, W. S. *Cooled cooling air systems for turbine thermal management*, presented at the International Gas Turbine & Aeroengine Congress & Exhibition, Indianapolis, IN, June 7−10, 1999; ASME Paper No. 99-GT-14; American Society of Mechanical Engineers: New York.

(2) Edwards, T.; Zabarnick, S. Supercritical fuel deposition mechanisms. *Ind. Eng. Chem. Res.* **1993**, *32*, 3117–3122.

(3) Yu, J.; Eser, S. Determination of critical properties (T_c, P_c) of some jet fuels. *Ind. Eng. Chem. Res.* **1995**, *34*, 404–409.

(4) Yamagata, K.; Nishikawa, K.; Hasegawa, S.; Fujii, T.; Yoshida, S. Forced convective heat transfer to supercritical water flowing in tubes. *Int. J. Heat Mass Transfer* **1972**, *15*, 2575–2593.

(5) Licht, J.; Anderson, M.; Corradini, M. Heat transfer and fluid flow characteristics in supercritical pressure water. *J. Heat Transfer, Trans. ASME* **2009**, *131*, No. 072502.

(6) Song, J. H.; Kim, H. Y.; Kim, H.; Bae, Y. Y. Heat transfer characteristics of a supercritical fluid flow in a vertical pipe. *J. Supercrit. Fluids* **2008**, *44*, 164–171.

(7) Jiang, P. X.; Zhang, Y.; Shi, R. F. Experimental and numerical investigation of convection heat transfer of CO_2 at supercritical pressures in a vertical mini-tube. *Int. J. Heat Mass Transfer* **2008**, *51*, 3052–3056.

(8) Jiang, P. X.; Zhang, Y.; Xu, Y. J.; Shi, R. F. Experimental and numerical investigation of convection heat transfer of CO_2 at supercritical pressures in a vertical tube at low Reynolds numbers. *Int. J. Therm. Sci.* **2008**, *47*, 998–1011.

(9) Jiang, P. X.; Zhang, Y.; Zhao, C. R.; Shi, R. F. Convection heat transfer of CO_2 at supercritical pressures in a vertical mini tube at relatively low Reynolds numbers. *Exp. Therm. Fluid Sci.* **2008**, *32*, 1628–1637.

(10) Bae, Y. Y.; Kim, H. Y. Convective heat transfer to CO_2 at a supercritical pressure flowing vertically upward in tubes and an annular channel. *Exp. Therm. Fluid Sci.* **2009**, *33*, 329–339.

(11) Hu, Z. H.; Chen, T. K.; Luo, Y. S.; Zheng, J. X.; Tang, M. Heat transfer characteristics of kerosene at supercritical pressure. *J. Xi'an Jiao Tong Univ.* **1999**, *33*, 62–65.

(12) Linne, D. L.; Meyer, M. L.; Edwards, T.; Eitman, D. A. *Evaluation of heat transfer and thermal stability of supercritical JP-7 fuel*; American Institute of Aeronautics and Astronautics, Inc. (AIAA): Reston, VA, 1997; No. 1997-3041.

(13) Zhong, F. Q.; Fan, X. J.; Yu, G.; Li, J. G.; Lu, X. N. *Heat Transfer of Aviation Kerosene at Supercritical Conditions*. Proceedings of the 44th AIAA/ASME/SAE/ASEE Joint Propulsion Conference & Exhibit, Hartford, CT; AIAA: Reston, VA, 2008; No. 2008-4615.

(14) Hitch, B.; Karpuk, M. *Experimental investigation of heat transfer and flow instabilities in supercritical fuels*; AIAA: Reston, VA, 1997; No. 1997-3043.

(15) Ernst, G.; Maurer, G.; Wiederuh, E. Flow calorimeter for the accurate determination of the isobaric heat capacity at high pressures; results for carbon dioxide. *J. Chem. Thermodyn.* **1989**, *21*, 53–65.

(16) Ernst, G.; Hochberg, U. G. Flow-calorimetric results for the specific heat capacity c_p of CO_2, of C_2H_6, and of $(0.5CO_2 + 0.5C_2H_6)$ at high pressures. *J. Chem. Thermodyn.* **1989**, *21*, 407–414.

(17) Ernst, G.; Philippi, R. Flow-calorimetric results for the specific heat capacity c_p of Water at pressures between 20 and 50 MPa and temperatures between 298.15 and 673.15 K. *J. Chem. Thermodyn.* **1990**, *22*, 211–218.

(18) Zhao, X. M.; Liu, Z. G.; Chen, Z. Q. Flow apparatus for measuring heat capacities of liquids and liquid mixtures at high pressure. *J. Shanghai Jiao Tong Univ.* **1999**, *33*, 1008–1012.

(19) Zhao, X. M.; Liu, Z. G.; Chen, Z. Q. Measurement device for heat capacities of HFC152a/HCFC22 liquid mixture. *J. Xi'an Jiao Tong Univ.* **1999**, *33*, 52−55, 63.

(20) Wagner, W.; Pruss, A. The IAPWS formulation 1995 for the thermodynamic properties of ordinary water substance for general and scientific use. *J. Phys. Chem. Ref. Data* **2002**, *31*, 387–535.

(21) Driesner, T. The system H_2O-NaCl. Part II: Correlations for molar volume, enthalpy, and isobaric heat capacity from 0 to 1000 degrees C, 1 to 5000 bar, and 0 to 1 X-NaCl. *Geochim. Cosmochim. Acta* **2007**, *71*, 4902–4919.

(22) Lemmon, E. W.; Span, R. Short fundamental equations of state for 20 industrial fluids. *J. Chem. Eng. Data* **2006**, *51*, 785–850.

(23) Magee, J. W.; Bruno, T. J.; Friend, D. G.; Huber, M. L.; Laesecke, A.; Lemmon, E. W.; Mclinden, M. O.; Perkins, R. A.; Baranski, J.; Widegren, J. A. *Thermophysical properties measurements and models for rocket propellant RP-1: Phase I*; NIST: Gaithersburg, MD, 2007; NISTIR 6646.

(24) Abdulagatov, I. M.; Azizov, N. D. Heat capacity of rocket propellant (RP-1 fuel) at high temperatures and high pressures. *Fuel* **2011**, *90*, 563–567.

(25) Huber, M. L.; Lemmon, E. W.; Ott, L. S.; Bruno, T. J. Preliminary surrogate mixture models for the thermophysical properties of rocket propellants RP-1 and RP-2. *Energy Fuels* **2009**, *23*, 3083–3088.

(26) Fan, X. J.; Yu, G. Analysis of thermophysical properties of Daqing RP-3 aviation kerosene. *J. Propul. Technol.* **2006**, *27*, 187–192.

(27) Deng, H. W.; Zhang, C. B.; Xu, G. Q.; Tao, Z.; Zhang, B.; Liu, G. Z. Density measurement of endothermic hydrocarbon fuel at sub- and supercritical conditions. *J. Chem. Eng. Data* **2011**, *56*, 2980–2986.

(28) Sun, Q. M.; Mi, Z. T.; Zhang, X. W. Determination of critical properties (t_c, p_c) of endothermic hydrocarbon fuels-RP-3 and simulated JP-7. *J. Fuel Chem. Technol.* **2006**, *34*, 466–470.